Isospin dependence of projectile fragmentation and neutron-skin thickness of neutron-rich nuclei*

MA Chun-Wang(马春旺)[1)] WANG Shan-Shan(王闪闪)

Department of Physics, Henan Normal University, Xinxiang 453007, China

Abstract: By investigating the cross section distributions of fragments produced in the 140 A MeV ^{40,48}Ca+^{9}Be and 1 A GeV ^{124,136}Xe+Pb reactions, the isospin dependence of projectile fragmentation in fragment production is studied. In the framework of the statistical abrasion-ablation model, the 1 A GeV ^{136}Xe+^{208}Pb reaction is calculated. By adjusting the diffuseness parameter in neutron density distribution of ^{136}Xe, we find the isospin dependence of projectile fragmentation in fragment production is sensitive to the neutron-skin thickness of the projectile nucleus.

Key words: heavy-ion collisions, isospin effect, projectile fragmentation

PACS: 21.65.Cd, 21.65.Ef, 25.70.Mn **DOI:** 10.1088/1674-1137/35/11/007

1 Introduction

Heavy-ion collisions (HICs) provide a lot of information about a nucleus far from the β-stability line. Nuclear reactions involving nuclei with a large neutron or proton excess can be studied at the built radioactive beam (RIB) facilities and the new generation of RIB facilities that are being constructed or planned, thus providing a great opportunity to study both the structure and other properties of isospin asymmetric nuclear matter that have large neutron/proton ratios. This has stimulated much interest and a lot of activities in a new research direction in nuclear physics, namely isospin physics [1]. A nucleus which has a large neutron/proton ratio is supposed to have a thick neutron-skin thickness (which is defined as the difference between the root-mean-square of the neutron and proton radii, i.e., $S_{\rm n} \equiv \langle r_{\rm n}^2\rangle^{1/2} - \langle r_{\rm p}^2\rangle^{1/2}$). The proton radius of a nucleus can be measured with very high accuracy through electron scattering [2]. But so far, the experimental accuracy of the neutron radius (and the neutron density) is much lower than that of the proton radius. Neutron-skin thickness is an important parameter constrained by symmetry energy and thus the equation of state (EOS) of a neutron-rich nucleus [3]. The constraint of $S_{\rm n}$ on EOS is important for improving our knowledge of neutron-rich matter and extrapolating the EOS to a higher neutron density [4–6], which makes $S_{\rm n}$ find its application in studying the property of neutron stars.

Different types of isospin phenomena in HICs, such as multifragmentation, fragment production, collective flow, pre-equilibrium nucleon emission, balance energy, etc., have been observed [7–15]. In Refs. [14, 15], the isospin dependence of projectile fragmentation in fragment production is discussed. In Ref. [16], the shift of centroids (or peak positions) of the fragment isotope distributions produced by symmetric projectile to neutron-rich projectiles is discussed. The production of neutron-rich fragments are affected by the neutron density distributions of a projectile nucleus. The relatively small shift in the peak positions of isotopic distributions is understood as the neutron-rich prefragments created in the fragmentation process decay toward the valley of stability. The similar density distributions of protons and neutrons in the core of a neutron-rich projectile nucleus account for a decreasing shift of centroids of the fragment isotopic distributions produced from asym-

Received 11 February 2011

* Supported by National Natural Science Foundation of China (10905017) and Program for Innovative Research Team (in Science and Technology) in University of Henan Province (2010IRTSTHN002), China

1) E-mail: machunwang@126.com

metric projectiles to neutron-rich projectiles [14, 15]. In this paper, one phenomenon of isospin dependence of projectile fragmentation, i.e., the shift of peak positions of the isotopic distributions produced in neutron-rich projectile fragmentation, and the correlation between this isospin phenomenon and neutron-skin thickness of projectile nuclei, will be discussed.

2 Model description

The statistical abrasion-ablation (SAA) model was developed by Brohm and Schmidt to describe HICs at high energies [17, 18]. It was modified by Fang et al. to describe HICs at intermediate energies [14, 15, 19–23]. The SAA model is used to predict fragment production in the projectile fragmentation in this paper.

A description of the SAA model can be found in Refs. [14, 17, 18, 23]. In the SAA model, a two-stage process is assumed in HICs. In the first collision stage, it takes independent N-N collisions for participants in an overlap zone of the two colliding nuclei and determines the distributions of abraded neutrons and protons.

The production cross section for a specific fragment in this stage is calculated from

$$\sigma(\Delta N,\Delta Z)=\int \mathrm{d}^2 b P(\Delta N,b)P(\Delta Z,b), \qquad (1)$$

where ΔN and ΔZ are the number of abraded neutrons and protons from the projectile; $P(\Delta N,b)$ and $P(\Delta Z,b)$ are the probability distributions for the abraded neutrons and protons at a given impact parameter b, respectively. These probability distributions are determined by a superposition of different binomial distributions. The density distributions of protons and neutrons are assumed to be the usually used Fermi-type,

$$\rho_{\mathrm{i}}(r)=\frac{\rho_{\mathrm{i}}^0}{1+\exp\left(\dfrac{r-C_{\mathrm{i}}}{f_{\mathrm{i}}t_{\mathrm{i}}/4.4}\right)}, \quad \mathrm{i}=\mathrm{n},\mathrm{p} \qquad (2)$$

where ρ_{i}^0 is the normalization constant; C_{i} is half the density radius of the neutron or proton density distribution; and t_{i} is the diffuseness parameter. f_{i} is introduced to adjust t_{i} and thus S_{n} [20, 22, 23].

The second stage is the evaporation process. In this stage, the residues in the first stage are de-excited and thermalized by the emission of neutrons, protons and other light particles in the way using a statistical model [17].

3 Results and discussion

The cross sections distributions of fragments produced in the 140 A MeV ^{40,48}Ca+^{9}Be [24] and 1 A GeV ^{124,136}Xe+Pb [25] will be investigated. The N/Z values of ^{40}Ca, ^{124}Xe, ^{48}Ca, and ^{136}Xe are 1, 1.3, 1.4 and 1.52, respectively, which form an N/Z chain. The isospin dependence of fragment production can be investigated in these four reactions.

In Fig. 1, the cross sections of fragments produced in the four reactions are plotted. First, we compare the cross sections of fragments produced by neutron-rich projectiles and symmetric projectile nuclei. For isotopes with a large charge number (Z_{f}), the cross sections of their neutron-rich side produced by neutron-rich projectiles are larger than those of symmetric projectiles. The peak positions of the isotopic distributions shift from those of symmetric projectiles to those of neutron-rich projectiles. It is the so-called phenomena of isospin dependence of fragment production in the neutron-rich nucleus projectile fragmentation [14, 15]. Second, we compare the cross sections of fragments produced in the four reactions, in which the projectile nuclei have different N/Z. For isotopes with Z_{f} approximately equal to Z_{p} (Z_{p} is the charge number of the projectile nucleus), the cross section distributions differ mostly in peak positions and widths. The peak positions of the isotopes that have relatively big N-Z and the width of the distributions are wider when the projectile nuclei have large N/Z. As Z_{f} decreases, the difference between the peak positions and the widths of the isotopic distributions decreases. For the isotopes with very small Z_{f} (for example, Z_{f}=14), the difference totally vanishes, as shown in the first panel of Fig. 1. This phenomenon is explained as the difference between neutron and proton density distributions in the core and surface of a neutron-rich nucleus [15].

The peak positions (P_{p}) and widths of the isotopic distributions in Fig. 1 are fitted using the Gaussian function. Values of P_{p} are plotted in Fig. 2(a). The P_{p} of isotopes produced both by ^{40,48}Ca and ^{124,136}Xe have big differences when $Z_{\mathrm{p}}-Z_{\mathrm{f}}$ is small. The difference between the P_{p} of isotopes produced by a neutron-rich projectile and a symmetric projectile become smaller and even overlap as Z_{f} decreases. As has been discussed in Refs. [14, 16], the P_{p} of the isotopes produced by a neutron-rich projectile shift to the neutron-rich side. To compare the shifts of these peak positions of the isotopes, the correlation between the neutron excess $(N-Z)_{\mathrm{s}}$ and the charge

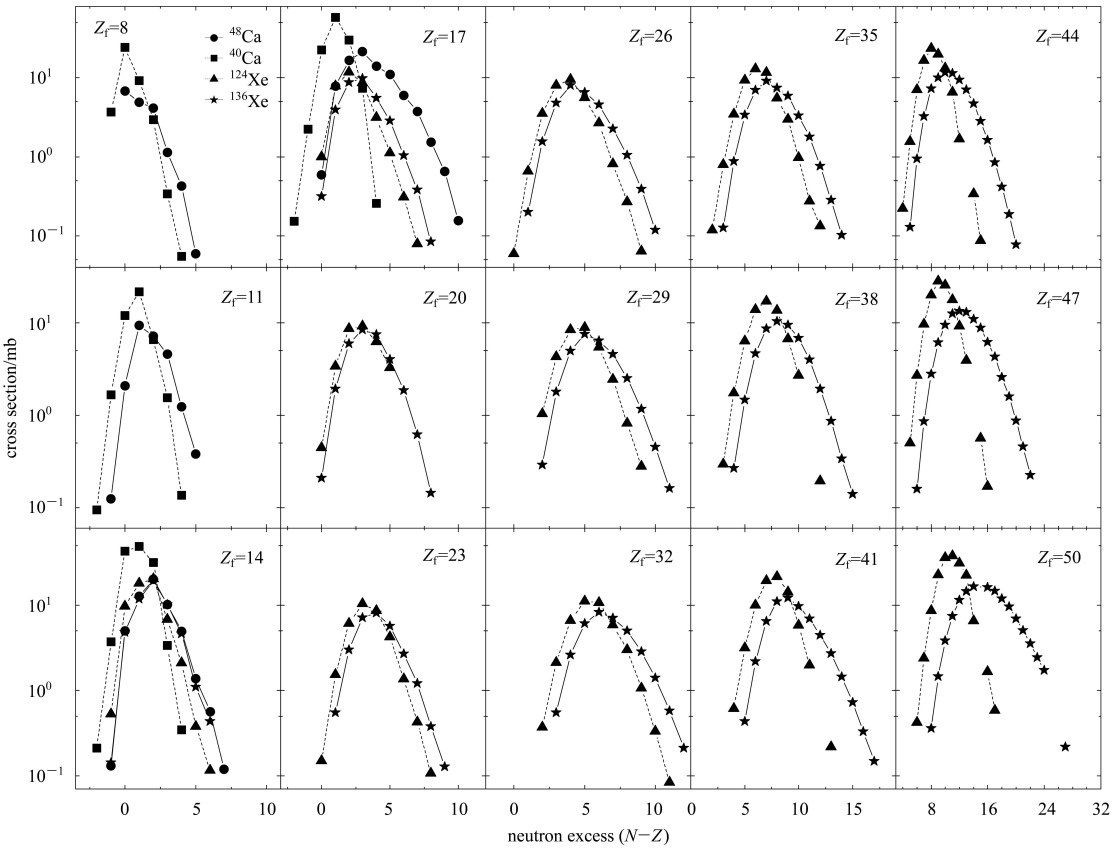

Fig. 1. The measured cross sections of fragments produced in the 140 A MeV ^{40,48}Ca+^{9}Be and the 1 A GeV ^{124,136}Xe + Pb reactions.

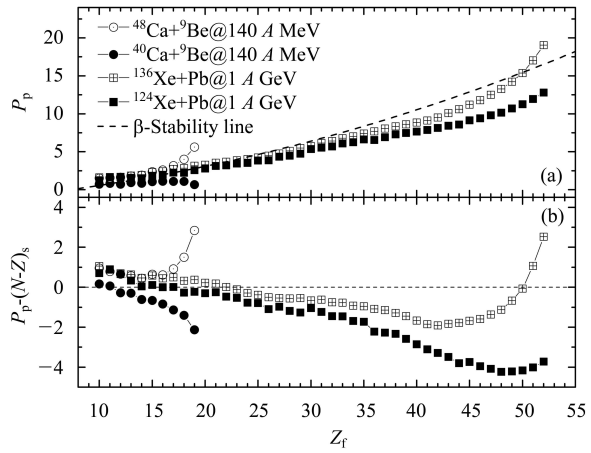

Fig. 2. (a) The peak positions (P_p) of isotopic distributions in the 140 A MeV ^{40,48}Ca + ^{9}Be and the 1 A GeV ^{124,136}Xe + Pb reactions. The dotted line is fitted from the neutron-proton correlation of nuclei at the β-stability line. (b) The difference between the P_p of isotopes [in (a)] and the values taken from the β-stability line ($(N-Z)_s$).

numbers of isotopes that locate at the β-stability valley (Z_s) is extracted. The $(N-Z)_s \sim Z_s$ correlation is plotted as the dashed line in Fig. 2(a). In Fig. 2(b) the difference between the P_p of isotopes and the values taken from the $(N-Z)_s \sim Z_s$ correlation of the β-stability line nuclei are plotted. While for the isotopes with small Z_f the P_p are near the β-stability line nuclei, the P_p of isotopes with large Z_f are smaller than the values of the β-stability line nuclei except for some isotopes produced by a very neutron-rich projectile.

In Fig. 3, the widths of the isotopic distributions in Fig. 1 are plotted. For ^{48}Ca and ^{146}Xe, the widths decrease as Z_f decreases. But the decreasing trend is very fast when $Z_p - Z_f$ is small and then slows down. For ^{40}Ca and ^{124}Xe, the widths decrease gradually as Z_f becomes smaller. The widths of the distributions overlap when Z_f is very small. The average value of these overlapping symbols is calculated (which is 2.0909) and plotted in Fig. 3 as a dashed line.

To investigate the isospin dependence of fragment production in projectile fragmentation, the 1 A GeV ^{136}Xe+^{208}Pb reaction is calculated using the SAA model. In the calculation, ^{208}Pb is taken as the target nucleus since the target is not specified in experiments. f_n is varied from 1.0 fm to 3.0 fm (in steps of 0.4 fm) to change the S_n of ^{136}Xe. The cross section distributions of fragments with Z <40 change little

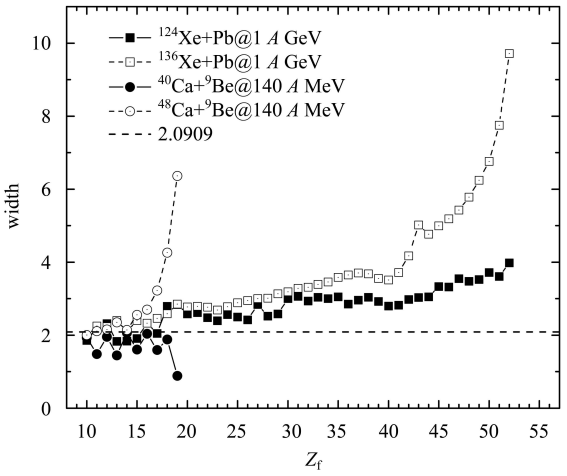

Fig. 3. The widths of fragment isotopic distributions produced in the 140 A MeV ^{40,48}Ca+^{9}Be and in the 1 A GeV ^{124,136}Xe+Pb reactions.

when f_n is altered. Since f_n mainly affects the density distributions of neutrons in the surface region, the change of f_n results in a different n/p ratio in this region of ^{136}Xe. According to the SAA model, the production of fragments in the first stage of the collision is determined by density distributions of protons and neutrons of projectile and target nuclei and nucleus-nucleus cross sections (σ_{NN}) [14, 15, 19]. Ignoring the density dependence of σ_{NN}, the big difference in the density distributions of protons and neutrons results in the isospin dependence of fragment production in the surface region of a nucleus.

In Fig. 4, the measured and calculated cross sections of fragments in 1 A GeV ^{136}Xe + ^{208}Pb are compared. The calculated cross sections of fragments can well reproduce the measured results when $Z_p - Z_f$ is not large. When $Z_p - Z_f$ increases, the calculated P_p becomes smaller than that of the measured results. The calculated cross sections of fragments with small Z_f differ mostly in the neutron-rich isotopes with large Z_f, which indicates that they are affected by f_n.

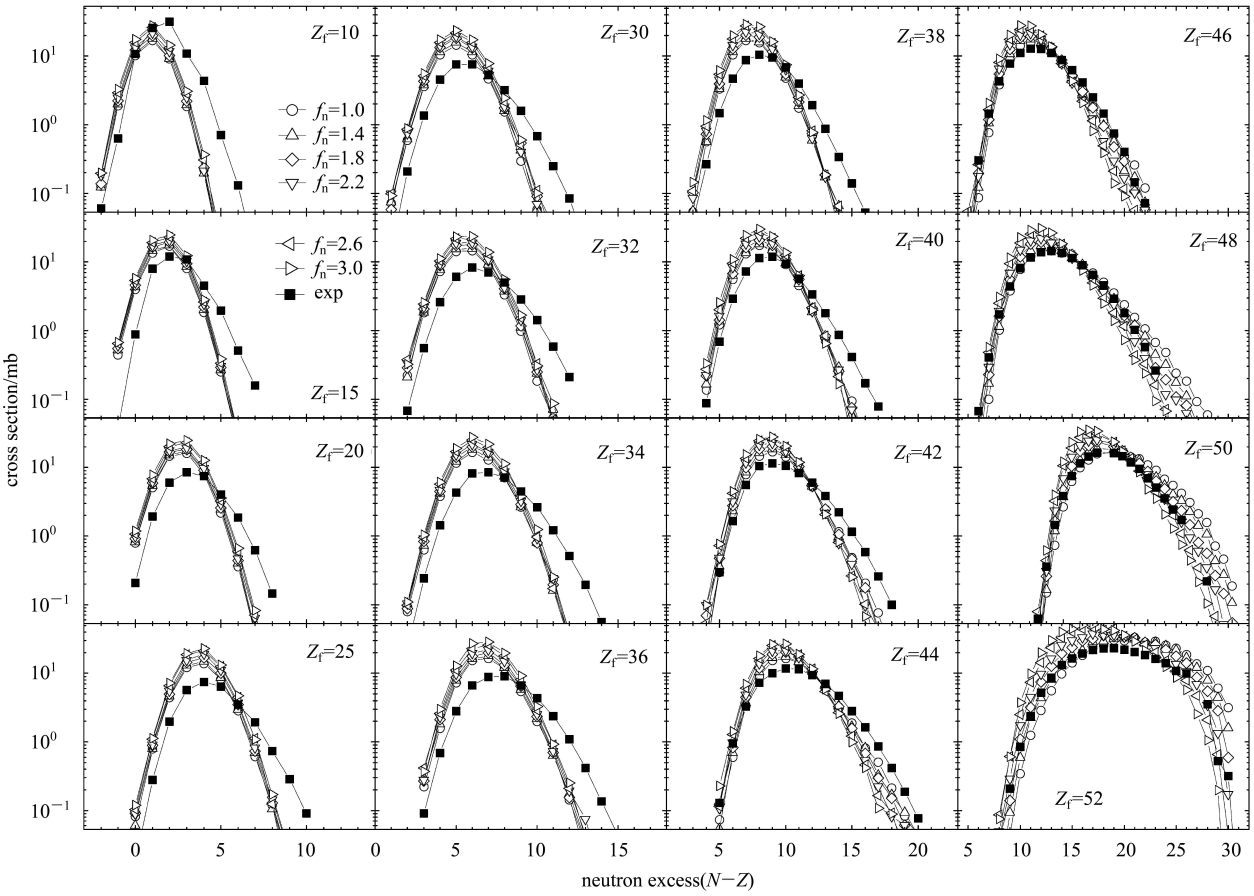

Fig. 4. The measured and calculated cross sections of fragments in 1 A GeV ^{136}Xe+^{208}Pb. f_n is varied from 1.0 to 3.0 in the calculations.

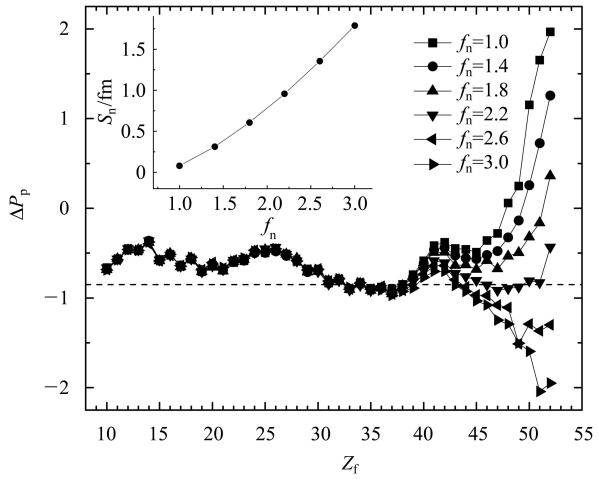

Fig. 5. $\Delta P_{\rm p}$ between the calculated and the experimental results in the 1 A GeV ^{136}Xe+^{208}Pb reaction. The inserted figure is the $S_{\rm n} \sim f_{\rm n}$ correlation of ^{136}Xe.

The calculated cross section distributions of fragments are also fitted using the Gaussian function. In Fig. 5, the difference between the $P_{\rm p}$ of isotope distributions calculated ($P_{\rm p}$(th)) and measured ($P_{\rm p}$(ex)), which is $\Delta P_{\rm p} = P_{\rm p}({\rm th}) - P_{\rm p}({\rm ex})$, are plotted. The difference is big only when $Z_{\rm p} - Z_{\rm f}$ is small. When $Z_{\rm f}$ <40, the difference is very small for different $f_{\rm n}$. Since $f_{\rm n}$ only adjusts the diffuseness of a nucleus and hardly changes density distributions in the core, the peak positions of the small $Z_{\rm p} - Z_{\rm f}$ isotopes are very sensitive to a density change at the surface region of the nucleus. The trend of $\Delta P_{\rm p}$ for large $Z_{\rm f}$ changes from increasing to decreasing when $f_{\rm n}$ is increased. $\Delta P_{\rm p}$ for $f_{\rm n}$ =2.2 becomes flat and indicates that $f_{\rm n}$ =2.2 is an appropriate value for ^{136}Xe. The inset figure in Fig. 5 shows the correlation between $S_{\rm n}$ and $f_{\rm n}$, which is a single-increasing function in the range shown. $S_{\rm n}$ of ^{136}Xe is 0.9566 fm when $f_{\rm n}$ =2.2. It should be pointed out that in Fermi-type density distribution, the parameter values will affect $S_{\rm n}$. Arbitrary parameters will introduce error in $S_{\rm n}$ theoretically.

4 Summary

In summary, the isospin dependence of fragment production in 140 A MeV ^{40,48}Ca and 1 A GeV ^{124,136}Xe projectile fragmentation is investigated. For a neutron-rich projectile nucleus, the peak positions of fragment isotopic distributions are located at more neutron-rich positions than those of symmetric projectiles. But this isospin phenomena becomes weak and even vanishes when the charge numbers of fragments decrease. To study the effect of neutron-skin thickness on this isospin phenomena, the cross sections of fragments produced by ^{136}Xe are calculated in the framework of the SAA model. When adjusting a parameter to change the diffuseness parameter of neutron density distribution and thus the neutron-skin thickness, it is found that the peak positions of fragment isotopic distributions are sensitive to the neutron-skin thickness of the projectile nucleus. Defining the difference between the peak positions of fragments for isotope distributions in theory and in experiment, it is found that the difference can serve as an observable to extract the neutron-skin thickness of a neutron-rich nucleus.

References

1 LI B A, Chen L W, Ko C M. Phys. Rep., 2008, **464**: 113
2 Fricke G, Bernhardt C, Heilig K et al. At. Data Nucl. Data Tables, 1995, **60**: 177
3 Tsang M B, Zhang Y, Danielewicz P et al. Phys. Rev. Lett., 2009, **102**: 122701
4 Brown B A. Phys. Rev. Lett., 2000, **85**: 5296
5 Yoshida S, Sagawa H. Phys. Rev. C, 2004, **69**: 024318
6 Furnstahl R J. Nucl. Phys. A, 2004, **706**: 85
7 MA Y G, SU Q M, SHEN W Q et al. Phys. Rev. C, 2000, **60**: 024607
8 Dempsey J F, Charity R J, Sobotka L G et al. Phys. Rev. C, 1996, **54**: 1710
9 LI B A, REN Z Z, Ko C M et al. Phys. Rev. Lett., 1996, **76**: 4492
10 Pak R, Benenson W, Bjarki O et al. Phys. Rev. Lett., 1997, **78**: 1022
11 Pak R, LI Bao-An, Benenson W, Bjarki O et al. Phys. Rev. Lett., 1997, **78**: 1026
12 CHEN L W, ZHANG F S, JIN G M. Phys. Rev. C, 1998, **58**: 2283
13 Miller M L, Bjarki O, Magestro D J et al. Phys. Rev. Lett., 1999, **82**: 1399
14 FANG D Q, SHEN W Q, FENG J et al. Phys. Rev. C, 2000, **61**: 044610
15 MA C W, WEI H L, WANG J Y et al. Chin. Phys. B, 2009, **18**: 4781
16 Lukyanov S, Mocko M, Andronenko L et al. Phys. Rev. C, 2009, **80**: 014609
17 Gaimard J J, Schmidt K -H. Nucl. Phys. A, 1991, **531**: 709
18 Brohm T, Schmidt K -H. Nucl. Phys. A, 1994, **569**: 821
19 MA C W, WEI H L, WANG J Y et al. Phys. Rev. C, 2009, **79**: 034606
20 MA C W, WEI H L, YU M. Phys. Rev. C, 2010, **82**: 057602
21 MA C W, WEI H L, LIU G J et al. J. Phys. G: Nucl. Part. Phys., 2010, **37**: 015104
22 FANG D Q, MA Y G, CAI X Z. Phys. Rev. C, 2010, **81**: 047603
23 MA C W, FU Y, FANG D Q et al. Chin. Phys. B, 2008, **17**: 1216
24 Mocko M, Tsang M B, Lacroix D et al. Phys. Rev. C, 2008, **78**: 024612
25 Henzlova D, Schmidt K H, Rricciardi M V et al. Phys. Rev. C, 2008, **78**: 044616